DEVELOPMENT OF SITE SPECIFIC AMPLIFICATION FACTORS

1.0 INTRODUCTION

Site specific amplification factors (5% damped pseudo absolute acceleration, Sa) for soil and firm rock profiles were developed for each site using equivalent-linear analyses for cases which had surficial materials with shear-wave velocity less than the hard rock reference value of 2.83 km/sec (9,285 ft/sec) and of sufficient thickness to impact design motions at frequencies below about 50 Hz. The conservative criteria used to qualify a site for development of site-specific amplification, defined as Sa of the site divided by Sa of reference rock, was more than 25 ft of material over hard rock with an average shear-wave velocity less than 7,500 ft/s. Site-specific amplification was developed for all sites not meeting the combined stiffness and velocity criteria. Epistemic uncertainty in dynamic material properties; shear-wave velocity profile, G/G_{max} and hysteretic damping, and total profile low strain damping (kappa; Anderson and Hough, 1984) was accommodated by development of multiple base-case models. For each base-case set of dynamic material properties, median and ± 1σ amplification factors were computed over a range in reference site loading levels. The aleatory variability about each base-case set of dynamic material properties was developed by randomizing (30 realizations) shear-wave velocities, layer thickness, depth to reference rock, and modulus reduction and hysteretic damping curves. For all the sites considered, where soil and rock extended to depths exceeding 500 ft, linear response was assumed (Silva et al.; 1996, 1998, 1999, 2000).

In all site response analyses motions were generated with the point-source model. The effects of control motion spectral shape on site amplification were examined conditional on reference site peak acceleration. The potential effects of both magnitude as well as single-verses double-corner (Atkinson and Boore, 1995) source spectra at large magnitude (**M** 6.5) were considered for a stiff soil profile. The results suggested the difference in amplification between single- verses double-corner source models were significant enough to consider the implied epistemic uncertainty in central and eastern North America (CENA) source processes at large magnitude (Section 3.1.2).

Considering magnitude, since the dominant contributions to the hazard across the central and eastern US. (CEUS) and oscillator frequency reflect magnitudes between about **M** 6.0 and **M** 7.5, the analyses suggested the use of a single magnitude of **M** 6.5 resulted in slightly conservative amplification (about 5%) for **M** 7.5 and a slight unconservative amplification (about 5 to 10%) for **M** 5.5 (Section 3.1.1). The difference between amplification computed for **M** 6.5 and both **M** 5.5 and **M** 7.5 were in the 5 Hz to 10 Hz frequency range and only at high loading levels of hard rock peak accelerations of 0.50g and above. In view of the little contribution of **M** 5.5 to the CEUS hazard, being dominated by about **M** 6.0 and larger, the use of a single magnitude of **M** 6.5 was adopted in lieu of two magnitudes, **M** 6.0 and **M** 7.5.

2.0 DEVELOPMENT OF BASE-CASE PROFILES AND ASSESSMENT OF EPISTEMIC UNCERTAINTY IN DYNAMIC MATERIAL PROPERTIES

In general a mean based approach was taken to accommodate epistemic uncertainty in dynamic material properties: shear-wave velocity profile, site material damping at low strain (parameterized through kappa), and modulus reduction and hysteretic damping

curves. In this context, for poorly characterized sites with few if any measured dynamic material properties, three profile estimates combined with three kappa estimates and two sets of modulus reduction and hysteretic damping curves results in eighteen sets of amplification factors for each magnitude. The three estimates for the shear-wave velocity profile and kappa were intended to capture uncertainty of the mean or best-estimate profile and kappa value and reflect the mean base-case as well as upper and lower range base-cases. A general set of guidelines was employed to develop base-cases for dynamic material properties as well as associated weights as given below.

2.1 Shear-Wave Velocity Profiles.

For sites with sparse information regarding dynamic material properties, e.g. shear-wave velocity profile was unavailable, typically an estimate based on limited surveys (e.g. compressional-wave refraction) was available over some shallow depth range. For such cases as well as to provide a basis for extrapolating profiles specified over shallow depths to hard rock basement material, a suite of profile templates was adopted, parameterized with $\overline{\mathbf{V}_s}$ (30m) ranging from 190m/s to 2,032m/s. The suite of profile templates is shown in Figure xx.1 to a depth of 1,000 ft. The templates were taken from Walling et al. (2008) supplemented for the current application with 190m/s, 1,364m/s, and 2,032m/s. The latter two profiles were added to accommodate residual soils (saprolite) overlying hard rock. For both soil and soft rock sites, the profile with the closest velocities over the appropriate depth range was adopted from the suite of profile templates and adjusted by increasing or decreasing the template velocities or, in some cases, stripping off material to match the velocity estimates provided.

For intermediate cases such as when only the upper portion of a deep soil profile is constrained with measured velocities, the closest template profile was used at the appropriate depth. The template was used to provide a rational basis to extrapolate the profile to the required depths.

For firm rock sites, which are typically Paleozoic sedimentary rocks such as shales, sandstones, siltstones, etc., the shear-wave velocity gradient of 0.5m/s/m from deep measurements in similar rocks in Japan (Fukushima et al., 1995) was adopted as a template and adjusted to the velocities provided over the appropriate depth range. The gradient of 0.5m/s/m is also consistent with sedimentary rocks of similar type at the Varian well in Parkfield, California (Jongmans and Malin, 1995). It is recognized the soil or firm rock gradients in the original profiles are primarily driven by confining pressure and may not be strictly correct for each adjusted profile template at each site. Any shortcoming in the assumed gradient is not expected to be significant as the range in multiple base-case profiles accommodates the effects of epistemic uncertainty in the profile gradient on amplification.

2.1.1 Epistemic Uncertainty, σ_μ

Profile epistemic uncertainty was taken as 0.35 (σ_μ ln) throughout the profile and was based on the estimates of epistemic uncertainty in $\overline{\mathbf{V}_s}$ (30m) (Chiou et al., 2008) for stiff profiles. The logarithmic factor assumes shear-wave velocities are lognormally distributed and was originally developed to characterize the epistemic uncertainty in measured $\overline{\mathbf{V}_s}$ (30m) at ground motion recording sites where measurements were taken at a maximum distance of 300m from the actual site. The uncertainty accommodates

spatial variability over maximum distances of 300m, and was adopted here as a reasonable and realistic uncertainty assessment reflecting a combination of few velocity measurements over varying depth ranges and shear-wave velocities inferred from compressional-wave measurements, in addition to the spatial variability associated with the velocities provided by the utilities. The application of the uncertainty estimate over the entire profile that is based largely on $\overline{\mathbf{V}_s}$ (30m) implicitly assumes perfect correlation that is independent of depth. While velocities are correlated with depth beyond 30m, which forms the basis for the use of $\overline{\mathbf{V}_s}$ (30m) as an indicator of relative site amplification over a wide frequency range, clearly the correlation is neither perfect nor remains high over unlimited depths (Boore et al., 2011).

The value of 0.35 adopted for profile epistemic uncertainty is also similar to the COV of 0.25 for shear-wave velocities over the top 50 to 75 ft found by Toro (Silva et al., 1996) for spatial variability over structural footprint dimensions of several hundred feet. In this case, based on measured profiles over a footprint, the COV decreased for depths beyond about 75 ft indicating less spatial variability with increasing depth. For the current application the value of 0.35 is retained with depth as the actual epistemic uncertainty is more appropriately considered to be depth independent as the uncertainty was intended to capture reasonable ranges in gradients.

More direct support for the assumption of a σ_μ of 0.35 comes from the measured range in ($\overline{\mathbf{V}_s}$ (30m) conditional on proxy inferences. For the four currently employed ($\overline{\mathbf{V}_s}$ (30m) proxies surficial geology (age; Wills and Silva, 1998, Wills and Clahan, 2006) Geomatrix site category (Chiou eat al., 2008), topographic slope (Wald and Allen, 2007), and

terrain (Yong et al., 2010), the overall within class or category uncertainty is about 0.35. This uncertainty reflects the variability of measured ($\overline{\mathbf{V}_s}$ (30m) about the predicted value and is relatively constant across proxies (Silva et al., 2012). The proxy uncertainty of about 0.35 is a direct measure of the uncertainty of the predicted value or estimate and supports the adoption of 0.35 to quantify the velocity uncertainty for cases with few or absent direct measurements. For the application to site characterization the σ_μ of 0.35 has been extended to the entire profile.

For cases where site-specific velocity measurements are particularly sparse, e.g. based on static tests for shear- and compressional-moduli, the uncertainty was increased to 0.50. The uncertainty was also increased to 0.50 in the absence of site-specific velocity measurements. For these cases the mean base-case profile was based on analogue materials from soil and rock descriptions provided by the utility. For the current application, where the desire was to implement a consistent approach to develop representative profiles and associated uncertainties to achieve mean based estimates of hazard, the assumption of a depth independent correlation is considered to reflect a sufficiently accurate approximation to the actual epistemic uncertainty.

2.1.2 Weights

To provide an expression of the epistemic uncertainty of a σ_μ (ln) of 0.35 in the final site-specific hazard, median amplification factors over thirty realizations expressing aleatory variability were computed for the base-case profile (mean base-case) as well as upper range and lower range base-cases. For scale factors and associated weights, to reflect a realistic uncertainty in the profile, the 90% level was adopted with a corresponding

profile scale factor of 1.3 σ_μ or 0.45. This represents an absolute factor of 1.57 on the mean base-case profile.

To accommodate the range in velocity profiles in terms of relative weights, the lower- and upper-range profiles were assumed to reflect 10^{th} and 90^{th} fractiles. The corresponding weights reflecting an accurate three point approximation of a normal distribution which preserves the mean are 0.30 for the 10^{th} and 90^{th} percentiles and 0.40 for the median (Keffer and Bodily, 1983) and summarized in Table xx.2. In the sections for each site relative weights are tabulated including any departures based on available site-specific information.

As an illustration Figure xx.2 shows the 560m/s base-case profile template (Figure xx.1) along with the expression of epistemic uncertainty as upper and lower ranges based on the scale factor of 0.45 (1.3 σ_μ). Also shown in Figure xx.2 is the firm rock gradient adopted from deep measurements of sandstones and siltstones in Japan of 0.5m/s/m (Fukushima et al., 1995). The assumed gradient is also consistent with that reflected in the Tertiary claystones, siltstones, sandstones, and conglomerates for measured shear-wave velocities at the Varian Well in Parkfield, California (Jongmans and Malin, 1995).

For the illustration the firm rock was taken to have an initial shear-wave velocity of 5,000 ft/s and the gradient was considered to reflect sedimentary rocks such as sandstones, siltstones, mudstone, and shales. In application the empirical gradient was simply scaled to reflect the shear-wave velocity and depth range specified for the particular site. If velocity information was lacking with only rock type specified, 5,000 ft/s was assumed at the surface and σ_μ taken as 0.5.

It is important to note for deep profiles, while the range in relative velocities is depth independent, the range in absolute velocity is large, accommodating a range in potential gradients as Figure xx.2 illustrates. For shallow profiles, at a shear-wave velocity of 1,000 ft/s, the lowest stiffness considered for siting a NPP, an uncertainty of 0.35 (scale factors of $1.3\sigma_\mu$) results in a considerable range in velocity from 633 ft/s to 1,576 ft/s. This velocity range reflects a range in elastic high-frequency amplification, relative to hard rock at 2.83 km/s of 3.8 to 2.4.

2.1.1.1 Sites With Intermediate Velocity Information

The profile σ_μ of 0.35 was adopted for cases of few if any measurements and reflects a maximum uncertainty. At the other extreme, for cases with complete and relatively recent (< 30 years) shear-wave velocity measurements throughout the entire profile, the epistemic uncertainty in shear-wave velocity was taken as zero.

For cases with intermediate or incomplete shear-wave velocity information, which reflects the majority of sites, the assessment of profile epistemic uncertainty was necessarily dependent on the mix of available profile information and based solely on judgment.

For the intermediate cases which, for example, shear-wave velocity inferred from in-situ compressional-wave measurements over extended portions of the profile (e.g. several hundred feet), σ_μ was divided by 2 with the corresponding scale factor of 1.29 σ_μ (1.26) to generate upper- and lower-range base-cases. For deeper depths the uncertainty was increased to 0.35 with offsets in the upper- and lower-range base-cases tapered to reduce the development of resonances.

2.2 G/Gmax and Hysteretic Damping Curves.

To characterize the epistemic uncertainty in nonlinear dynamic material properties for both soil and firm rock sites, two sets of modulus reduction and hysteretic damping curves were used.

For soils, the two sets of curves used were EPRI (1993) and Peninsular Range (Silva et al., 1996; Walling et al., 2008). The two sets of generic curves are appropriate for cohesionless soils comprised of sands, gravels, silts, and low plasticity clays. The EPRI (1993) curves, illustrated in Figure xx.3, were developed for application to CENA sites and display a moderate degree of nonlinearity. The EPRI (1993) curves are depth (confining pressure) dependent as shown in Figure xx.3.

The Peninsular Range curves reflect more linear cyclic shear strain dependencies than the EPRI (1993) curves (Walling et al., 2008) and were developed by modeling recorded motions as well as empirical soil amplification in the Abrahamson and Silva WNA (Western North America) GMPE (Silva et al., 1996; Abrahamson and Shedlock, 1997). The Peninsular Range curves reflect a subset of the EPRI (1993) soil curves with the 51 ft to 120 ft EPRI (1993) curves applied to 0 ft to 50 ft and EPRI (1993) 501 ft to 1,000 ft curve applied to 51 ft to 500 ft.

The two sets of soil curves were considered to reflect a realistic range in nonlinear dynamic material properties for cohesionless soils. The use of these two sets of cohesionless soil curves implicitly assumes the soils considered do not have response dominated by soft and highly plastic clays or coarse gravels or cobles. The presence of relatively thin layers of hard plastic clays are considered to be accommodated with the

more linear Peninsular Range curves while the presence of gravely layers are accommodated with the more nonlinear EPRI (1993) soil curves, all on a generic basis.

The two sets of soil curves were given equal weights (Table xx.2) and are considered to represent a reasonable accommodation of epistemic uncertainty in nonlinear dynamic material properties for the generic types of soils in CEUS (Central and Eastern U.S.):

1. Glaciated regions which consist of both very shallow Holocene soils overlying tills as well as deep soils such as the Illinois and Michigan basins, all with underlying either firm rock (e.g. Devonian Shales) and then hard basement rock or simply hard basement rock outside the region of Devonian Shales,
2. Mississippi embayment soils including loess,
3. Atlantic and Gulf coastal plain soils which may include stiff hard clays such as the Cooper Marl,
4. Residual soils (saprolite) overlying hard metamorphic rock along the Piedmont and Blue Ridge physiographic regions.

To illustrate the difference in amplification between the EPRI (1993) and Peninsular Range cohesionless soil curves, Figure xx.4 shows estimates of median amplification factors (5% damped Sa) computed for template profile 400m/s (Figure xx.1) and a depth of 500 ft to basement rock using both sets of curves. In Figure xx.4 hard reference rock loading levels range from 0.01g to 1.50g (Table xx.1) and shows significantly greater nonlinear effects for the EPRI (1993) compared to the Peninsular Range curves at high frequency (≥ 2 Hz).

For firm rock, taken generally as Paleocene sedimentary rocks, such as shales, sandstones, siltstones, etc., two expressions of nonlinear dynamic material properties were assumed: EPRI rock curves (Figure xx.5) and linear response. The EPRI rock curves were developed during the EPRI (1993) project by assuming firm rock, with nominal shear-wave velocities in the range of about 3,000 ft/s to about 7,000 ft/s (about 5,000 ft/s on average), behaves in a manner similar to gravels (EPRI, 1993) being significantly more nonlinear with higher damping than more fine grained sandy soils. The rock curves were not included in the EPRI report as the final suite of amplification factors was based on soil profiles intended to capture the behavior of soils ranging from gravels to low plasticity sandy clays at CEUS nuclear power plants. With the stiffness typically associated with consolidated sedimentary rocks, cyclic shear strains remain relatively low compared to soils with significant nonlinearity confined largely to the very high loading levels (e.g. ≥ 0.75g).

As an alternative to the EPRI rock curves, linear response was assumed. Implicit in this model is purely elastic response accompanied with damping that remains constant with cyclic shear strain at loading levels up to and beyond 1.5g (reference site). Note in all cases the amplification at 1.5g was applied at higher loading levels.

Similar to the two sets of curves for soils, equal weights were given to the two sets of nonlinear properties for firm rock as summarized in Table xx.2.

2.3 Kappa

In the context of this report the kappa referred to is the profile damping contributed to by both intrinsic hysteretic damping as well as scattering due to wave propagation in

heterogeneous material. Both the hysteretic intrinsic damping and the scattering damping within the profile and apart from the crust are assumed to be frequency independent, at least over the frequency range of interest for Fourier amplitude spectra (0.33 Hz to about 25.0 Hz). As a result the kappa estimates reflect values that would be expected to be measured based on empirical analyses of wavefields propagating throughout the profiles at low loading levels and reflects the effective damping or "effective" Q_S within the profile (Campbell, 2009).

2.3.1 Low Strain Kappa For Rock Sites

Mean base-case kappa values were developed differently for soil and firm rock sites. For rock sites with at least 3,000 ft of firm sedimentary rock ($\overline{\mathbf{V}_s}$ (30m) > 500m/s) overlying hard rock, the kappa $\overline{\mathbf{V}_s}$ (100 ft) relation of

$$\kappa = 2.2189 - 1.0930 \log (\overline{\mathbf{V}_s} (100 \text{ ft})) \qquad \text{(Equation 1)}$$

was used to assign a mean base-case estimate for kappa (Silva et al., 2000; Van Houtte et al., 2011). The requirement of 3,000 ft reflects the assumption that the majority of damping contributing to kappa occurs over the top 3,000 ft with a minor contribution from deeper materials, e.g. 0.006s for hard rock basement material. As an example for a firm sedimentary rock with a shear-wave velocity of 5,000 ft/s Equation 1 gives a kappa estimate of about 0.02s. The assumption implies a kappa of 0.014s is contributed by the sedimentary rock column, 0.006s from the underlying reference rock (Table xx.1), and reflects an average Q_S of about 40 over 3,000 ft. The Q value of 40 for sedimentary rocks is consistent with the average value of 37 over the depth range of 0m to 298m in Tertiary claystones, siltstones, sandstones, and conglomerates at a deep

borehole in Parkfield, California (Jongmans and Malin, 1995). The average shear-wave velocity of about 4,800 ft/s (Campbell, 2009) is somewhat below the assumed base-case average of about 5,600 ft/s but well within the epistemic uncertainty (Figure xx.2).

For low firm rock velocities an upper bound kappa value of 0.04s was imposed. The maximum kappa value of about 0.04s reflects a conservative average for soft rock conditions (Silva and Darragh, 1995; Silva et al., 1996).

For cases where the thickness of firm rock was less than about 3,000 ft, kappa contributed by the firm rock profile was computed assuming a Q_s of 40 plus the contribution of the reference rock profile of 0.006s (Table xx.1a). For the three base-cases firm rock profiles shown in Figure xx.2, the total kappa values assuming a Q_s of 40 are 0.019s, 0.025s, and 0.015s for the mean, lower range, and upper range base-cases respectively.

2.3.2 Low Strain Kappa For Soil Sites

For soil sites with depths exceeding 3,000 ft to hard rock, a mean base-case kappa of 0.04s was assumed based upon average values for deep soil sites and low loading levels. The mean base-case kappa of 0.04s adopted for deep firm soils is lower than the value of approximately 0.06s based on recordings at alluvium sites located in Southern California (Anderson and Hough, 1984; Silva et al., 1996). For soil sites, due to nonlinear effects, low strain kappa may be overestimated depending upon loading level and the nonlinear dynamic material properties. To avoid potential bias in the deep firm soil low strain kappa, the value of 0.04s was based on inversions of the Abrahamson and Silva (1997) soil site GMPE (Silva et al., 1996). In that inversion a

range of rock site loading levels was used with the soil value of 0.04s based upon a rock site peak acceleration of 5%g or less, clearly a low strain estimate. The deep soil mean base-case kappa of 0.04s was adopted for both the upper and lower range profiles with the assumption the suite of profiles reflect deep firm soils. The assumed kappa of 0.04s for deep (≥ 3,000 ft) firm soils in the CEUS is somewhat less than the 0.054s inferred by Campbell (2009) based on Cramer et al. (2004) analyses for effective Q_s within the 960m deep sedimentary column in the Mississippi embayment near Memphis, Tennessee. The deep firm soil kappa of 0.04s is in fair agreement with 0.052s found by Chapman et al. (2003) for the 775m thick sedimentary column near Summerville, South Carolina.

In summary, for deep firm soil sites (≥ 3,000 ft) in the CEUS, a nominal kappa value of 0.04s based on an average of many empirical estimates predominately in the WNA tectonic regime was adopted. Sparse analyses for deep soil sites in the CEUS suggest 0.04s reflects some conservatism. However it should be noted the small strain total kappa is rapidly exceeded as loading level increases due to nonlinear response. The initial low strain kappa serves primarily as a means of adjusting (lowering) kappa to accommodate the scattering component due to the profile randomization.

For cases of shallower soils, less than 3,000 ft to hard rock basement material, the empirical relation of Campbell (2009) was used for the contribution to kappa from the sediment column (H)

$$\kappa(ms) = 0.0605 * H(m) \qquad \text{(Equation 2).}$$

The basement kappa value of 0.006s (Table xx.1a) in lieu of Campbell's (2009) estimate of 0.005s was added to the sediment contribution to estimate the total kappa.

For 3,000 ft (1 km) of soil, Campbell's (2009) relation predicts a total kappa of 0.066s, considerably larger than the mean base-case value of 0.04s, suggesting a degree of conservatism at low loading levels for CENA firm soils. For continuity, in the implementation of Equation 2, a maximum kappa of 0.04s was implemented for sites with less than 3,000 ft of firm soils.

The final class of soils considered comprises soils over firm rock with a total (firm rock plus soil) thickness of less than 3,000 ft. For these cases the appropriate soil or firm rock approaches outlined above were applied.

Additionally, for these relatively shallow soil/shallow rock sites, a global maximum kappa for the mean base-case was taken as 0.04s, slightly lower than the average low strain value based on a large sample of WNA analyses (Anderson and Hough, 1984; Silva and Darragh, 1995).

2.3.1 Epistemic Uncertainty

Epistemic uncertainty in kappa was taken as 50% (σ_μ = 0.40, Table xx.2; EPRI, 1993) about the mean base-case estimate. The uncertainty is based on the variability in kappa determined for rock sites which recorded the 1989 **M** 6.9 Loma Prieta Earthquake (EPRI, 1993), and adopted here as a reasonable expression of epistemic uncertainty at a given site. As with the profiles (Section 2.1), the 1.68 (1.3 σ_μ) variation is considered to reflect 10% and 90% fractiles with weights of 0.30 and a weight of 0.40 for the mean base-case estimate. The models for epistemic uncertainty are summarized in Table xx.2.

2.4 Densities

Because relative (soil surface/reference site) densities play a minor role in site-specific amplification, a simple model based on shear-wave velocity of the mean base-case profile was implemented for cases where profile density was not specified:

Shear-Wave Velocity (m/s)	Density (g/cm^3)
< 500	1.84
500 to 700	1.92
700 to 1,500	2.10
1,500 to 2,500	2.20
> 2,500	2.52

Due to the square root dependence of amplification on the relative density, a 20% change in soil density results in only a 10% change in amplification and only for frequencies at and above the column resonant frequency. As a result only an approximate estimate of profile density was considered necessary with the densities of the mean base-case profile held constant for the upper and lower range base-case profiles. This approach was a means of accommodating epistemic uncertainty in both density as well as shear-wave velocity (Section 2.1.1) in the suite of analyses over velocity uncertainty.

3.0 DEVELOPMENT OF AMPLIFICATION FACTORS

To develop amplification factors, the Mid-continent crustal model (EPRI, 1993) with a shear-wave velocity of 2.83 km/sec, a defined shallow crustal damping parameter (kappa; Anderson and Hough, 1984) of 0.006 sec, and a frequency dependent deep crustal damping Q model of 670 $f^{0.33}$ (EPRI, 1993) (Table xx.1a) was used to compute reference motions (5% damped pseudo absolute acceleration spectra). The Q(f) kappa, and reference site shear-wave velocities are consistent with the EPRI GMPEs (Ground

Motion Prediction Equations) (EPRI, 2004) and the site-specific profiles were simply placed on top of this defined crustal model which has a reference shear-wave velocity of 2.83 km/sec (≈ 9,300 ft/sec) and a reference kappa value of 0.006 sec. Distances were determined to generate a suite of reference site motions with expected peak acceleration values which cover the range of spectral accelerations (at frequencies of 0.5, 1.0, 2.5, 5.0, 10.0, 25.0, 100.0 Hz) anticipated at the sites analyzed. To cover the range in loading levels, 11 expected (median) peak acceleration values at reference rock (shear-wave velocity of 2.83 km/s, kappa = 0.006s; Table xx.1) were run from 0.01g to 1.50g (Table xx.1).

Amplification factors (5% damping response spectra) were then developed by placing the site profile on the Mid-continent crustal model at each distance, generating soil motions, and taking the ratios of site-specific response spectra (5% damped) to hard rock reference site response spectra. For the higher levels of rock motions, above about 1 to 1.5g for the softer profiles, the high frequency amplification factors were significantly less than 1, which may be exaggerated. To adjust the factors for these cases an empirical lower bound of 0.5 was implemented (EPRI, 1993; Abrahamson and Silva, 1997).

3.1 Effects of Control Motion Spectral Shape on Amplification

Conditional on reference site peak acceleration, amplification factors depend, to some extent, upon control motion spectral shape due to nonlinear response. For the same reference site peak acceleration, amplification factors developed with control motions reflecting **M** 5.5 will differ somewhat with those developed using a larger or smaller magnitude.

The other potential issue regarding control motion spectral shape that may affect amplification is the potential for CENA source processes to reflect a significant spectral sag at large magnitude (**M** ≥ 6) and intermediate frequency (Atkinson and Boore, 1995), compared to source processes of tectonically active regions. Such a trend was suggested by the 1988 **M** 5.9 Saguenay, Canada and 1985 **M** 6.8 Nahanni, Canada earthquakes. As a result, a simple source model was developed to characterize the potential for CENA large magnitude source spectra to reflect an intermediate frequency departure from the single-corner frequency point-source model (Boore, 1983). The two-corner source model for CENA (Atkinson and Boore, 1995) manifests the spectral sag between two empirical corner frequencies which are dependent on magnitude. The two-corner model merges to the single-corner model for **M** less than about **M** 5 with the depth and width of the spectral sag increasing with magnitude. Interestingly the two-corner model has been implemented for tectonically active regions and shown to be more representative of WNA source processes than the single-corner model (Atkinson and Silva, 2000), albeit with a much less pronounced spectral sag than the CENA model.

3.1.1 Effects of Magnitude on Amplification

Figure xx.6 shows amplification factors developed for profile 400m/s (Figure xx.1) using the single-corner source model for magnitudes **M** 5.5, 6.5, and 7.5. For this sensitivity analysis the more nonlinear EPRI G/G_{max} and hysteretic damping curves (Figure xx.3) were used as dependence on control motion spectral shape decreases with degree of nonlinearity becoming independent for linear analyses. As Figure xx.6 illustrates, the largest amplification reflects the lowest magnitude. Over the frequency range of about 5

Hz to 10 Hz, the largest range in amplification is about 20% and at the higher loading levels (≥ 0.75g). The largest difference in amplification is between **M** 5.5 and **M** 6.5 with little difference (< 10%) between **M** 6.5 and **M** 7.5. With the current source characterization in CENA and distribution of sites, the dominant contribution for the annual exceedence frequencies (AEF) of 10^{-4} and below are from magnitudes in the range of about **M** 6 to **M** 7+. As a result, to reduce the analyses to a manageable level, a single magnitude **M** 6.5 was selected to adequately characterize the amplification, with tacit acceptance of slight conservatism for magnitude contributions above about **M** 7.

3.1.2 Effects of Single-Verses Double-Corner Control Motion Spectral Shape On Amplification

One- and two-corner (Atkinson and Boore, 1995) source models were also used for **M** 6.5. While neither the single- or two-corner source models alone are considered appropriate for CENA (Central and Eastern North America) sources due to a lack of observations for **M** > 6, the two models were considered to reflect a reasonable range in spectral composition for large magnitude CENA sources. As a result equal weights were selected as shown in Table xx.2 for amplification factors developed using each source model. Additionally, for moderately stiff soils, typical for NPP siting, the difference in amplification between single- and double-corner source models becomes significant only at the higher loading levels as Figure xx.7 illustrates as an example. For profile 400m/s Figure xx.6 compares the amplification computed for both as single- and double-corner source models and EPRI modulus reduction and hysteretic damping curves (Figure xx.3), the most nonlinear set of curves for soils. As Figure xx.7 shows, for loading levels up to about 0.5g (reference rock median peak acceleration), the

difference in amplification is maximum around 10 Hz and in the 10% to 15% range, at higher loading levels the differences increase and become more significant.

Considering three profiles, three low-strain kappa values, two sets of G/G_{max} and hysteretic and hysteretic damping curves along with two magnitudes using both single- and double-corner source models results in a maximum of seventy two sets of amplification factors for poorly characterized sites. Accommodation of epistemic uncertainty in dynamic material properties reflects a computationally intense process unless consideration is given to a statically based selection approach such as Latin Hypercubes. Alternatively the number of models to characterize the epistemic uncertainty in dynamic material properties and source processes can be reduced. Reducing the number of magnitudes from two to one reduces the suite of amplification factors from 72 to 36 (Table xx.3). Further consideration of the sensitivities of source and site uncertainties on amplification can substantially reduce the number of models. For soils, since low strain kappa is only operational at the lowest loading levels as nonlinearity controls the effective damping throughout the nonlinear section (maximum of 500 ft) of the profile, multiple kappa values are redundant for practical applications. For soil sites overlying hard rock, the practical number of models required to characterize source and site epistemic uncertainty is reduced to 12 as shown in Table xx.3.

For firm rock sites, kappa represents a controlling parameter even for the nonlinear case using rock G/G_{max} and hysteretic damping curves (Figure xx.5) as the increase in kappa only occurs at very high loading levels due to the relatively high shear-wave velocities (Figure xx.2). For firm rock site conditions, since significant nonlinearity is

expected only at very high loading levels, the effects of single-verses double corner source models are small, only the single-corner model was run, reducing the number of models to 18 (Table xx.3). For cases where firm rock shear-wave velocities were high, exceeding about 7,000 ft/s, only linear analyses were run further reducing the model count to 9.

Finally, the most computationally intense case was for soil overlying firm rock. To fully capture the range in epistemic uncertainty in both the soil as well as firm rock, the maximum model count was 36 (Table xx.3).

In all the cases for site type, soil, firm rock, and soil plus firm rock, available site-specific information and judgment conditioned the actual number of cases analyzed. In general emphasis was placed on adequately characterizing the epistemic uncertainty on a case-by- case basis.

4.0 ALEATORY VARIABILITY IN DYNAMIC MATERIAL PROPERTIES

To accommodate aleatory variability in dynamic material properties expected to occur across each site (footprint), shear-wave velocity profiles as well as G/Gmax and hysteretic damping curves were randomized. Since depth to hard rock material (defined as shear-wave velocity of 2.83 km/sec (9,285 ft/sec)) is poorly known at many deep soil and firm rock sites, it was taken at a large enough depth to accommodate maximum amplification to the lowest frequency of interest, 0.33 Hz (Silva et al., 1999, 2000). For these cases, basement depth was randomized over a range of ± 30% of the best-estimate depth to accommodate aleatory variability about the median amplification and to smooth over potential low-frequency resonances. For sites where depth to basement

was relatively well known, perhaps from nearby well logs, a more restrictive range of ± 20% was used. In all cases, the basement depth randomization assumed a uniform distribution (EPRI, 1993).

The profile randomization scheme, which varies both layer velocity and thickness, is based on a correlation model developed from an analysis of variance of about 500 measured shear-wave velocity profiles (EPRI, 1993; Silva et al., 1996). This model uses variability in velocity that is appropriate for a large structural footprint. The parametric variation includes profile velocity and layer thickness variation as well as depth to hard rock material (2.83 km/sec). To prevent unrealistic velocity realizations, a bound of ± 2σ was placed throughout the profile. For the footprint correlation model the empirical σ is about 0.25 and decreases with depth to about 0.15 below about 50 ft (Silva et al., 1996).

To accommodate aleatory variability in the modulus reduction and hysteretic damping curves on a generic basis, the curves were independently randomized about the base case values (Section 2.0). A log normal distribution was assumed with a σ_{ln} of 0.15 and 0.30 at a cyclic shear strain of 3×10^{-2}% for modulus reduction and hysteretic damping respectively (Silva et al., 1996) with upper and lower bounds of 2σ. The truncation is necessary to prevent modulus reduction or damping models that are not physically realizable. The distribution is based on an analysis of variance of measured G/G_{max} and hysteretic damping curves and is considered appropriate for applications to generic (material type specific) nonlinear properties (Silva et al., 1996). The random curves were generated by sampling the transformed normal distribution with a σ_{ln} of 0.15 and 0.30 as appropriate, computing the change in normalized modulus reduction or percent

damping at 3 x 10^{-2}% cyclic shear strain, and applying this factor at all strains. The random perturbation factor was reduced or tapered near the ends of the strain range to preserve the general shape of the base-case curves (Silva, 1992; EPRI, 1993). Also, damping was limited to a maximum value of 15% in this application for NPPs.

To accommodate epistemic uncertainty in dynamic material properties (Section 2.0), multiple base-case (mean) models were considered, each with associated aleatory variability captured by the randomization process. Amplification factors for each case of epistemic uncertainty in dynamic material properties were then expressed as median and $\pm$ 1σ estimates based on 30 realizations at each distance or reference site loading level (Silva et al., 1999; 2000). Final hazard was developed by weighting over exceedence frequencies computed for each base-case model.

REFERENCES

Abrahamson, N.A and K.M. Shedlock (1997). "Overview." *Seis. Research Lett.,* 68(1), 9-23.

Abrahamson, N.A. and Silva, W.J. (1997). "Empirical response spectral attenuation relations for shallow crustal earthquakes." *Seism. Res. Lett.,* 68(1), 94-127.

Anderson, J. G. and S. E. Hough (1984). "A Model for the Shape of the Fourier Amplitude Spectrum of Acceleration at High Frequencies." *Bull. Seism. Soc. Am.,* 74(5), 1969-1993.

Atkinson, G. M., and D. M. Boore (1995). "New ground motion relations for eastern North America." *Bull. Seism. Soc. Am*. 85, 17–30. 12.

Boore, D.M. (1983). "Stochastic simulation of high-frequency ground motions based on seismological models of the radiated spectra." *Bull. Seism. Soc. Am.,* 73(6), 1865-1894.

Boore, D.M., E.M. Thompson, and H. Cadet (2011). "Regional correlations of V_{S30} and velocities averaged over depths less than and greater than 30m." *Bull. Seism. Soc. Am.,* in-press.

Campbell, K. W. (2009). "Estimates of shear-wave *Q* and κ_o for unconsolidated and semiconsolidated sediments in Eastern North America." *Bull. Seism. Soc. Am,* 99(4), 2365-2392.

Chapman, M. C., P. Talwani, and R. C. Cannon (2003). Ground-motion attenuation in the Atlantic Coastal Plain near Charleston, South Carolina, *Bull. Seism. Soc. Am.,* 93, 998–1011.

Chiou, B., R. Darragh, N. Gregor, and W. Silva (2008). "NGA project strong-motion database." *Earthquake Spectra*, **24**: 23-44.

Cramer, C. H., J. S. Gomberg, E. S. Schweig, B. A. Waldron, and K. Tucker (2004). The Memphis, Shelby Country, Tennessee, seismic hazard maps, *U.S. Geol. Surv.* Open-File Rept. 04-1294.

Electric Power Research Institute (2004). "CEUS Ground Motion Project" Palo Alto, Calif: Electric Power Research Institute, Final Report.

Electric Power Research Institute (1993). "Guidelines for determining design basis ground motions." Palo Alto, Calif: Electric Power Research Institute, vol. 1-5, EPRI TR-102293.

vol. 1: Methodology and guidelines for estimating earthquake ground motion in

eastern North America.
vol. 2: Appendices for ground motion estimation.
vol. 3: Appendices for field investigations.
vol. 4: Appendices for laboratory investigations.
vol. 5: Quantification of seismic source effects.

Fukushima, Y., J.C. Gariel, and R. Tanaka (1995). "Site-Dependent Attenuation Relations of Seismic Motion Parameters at Depth Using Borehole Data." *Bull. Seism. Soc. Am.*, 85(6), 1790-1804.

Jongmans, D. and P.E. Malin (1995). "Microearthquake S-wave Observations from 0 To 1 km in the Varian Well at Parkfield, California." *BSSA,* 85(6), 1805-1820.

Keefer D. I. and Bodily, S. E. (1983). "Three-point approximations for continuous random variables" *Management Science*, 2(5), 595-695.

Houtte, C.V., S. Drouet, and F. Cotton (2011). “Analysis of the origins of κ (kappa) to compute hard rock to rock adjustment factors for GMPEs.” *Bull. Seism. Soc. Am.,* v.101, p. 2926-2941.

Silva, W. J., E. Thompson, H. Magistrale, C. Wills (2012). “Development of a $\overline{V_S}$ (30m) map for central and eastern north america (cena): median estimates and uncertainties.” FM Global final report.

Silva, W.J., R. Darragh, N. Gregor, G. Martin, C. Kircher, N. Abrahamson (2000). “Reassessment of site coefficients and near-fault factors for building code provisions.” Final Report *USGS Grant award* #98-HQ-GR-1010.

Silva, W. J.,S. Li, B. Darragh, and N. Gregor (1999). "Surface geology based strong motion amplification factors for the San Francisco Bay and Los Angeles Areas."A PEARL report to PG&E/CEC/Caltrans, Award No. SA2120-59652.

Silva, W.J. Costantino, C. Li, Sylvia (1998). “Quantification of nonlinear soil response for the Loma Prieta, Northridge, and Imperial Valley California earthquakes.” Proceedings of The Second International Symposium on The effects of Surface Geology on Seismic Motion Seismic Motion/Yokohama/Japan/1-3 December 1998, Irikura, Kudo, Okada & Sasatani (eds.), 1137—1143.

Silva, W.J., N. Abrahamson, G. Toro and C. Costantino. (1996). “Description and validation of the stochastic ground motion model." Report Submitted to Brookhaven National Laboratory, Associated Universities, Inc. Upton, New York 11973, Contract No. 770573.

Silva, W.J., and R. Darragh, (1995). "Engineering characterization of earthquake strong ground motion recorded at rock sites." Palo Alto, Calif.: Electric Power Research Institute, Final Report RP 2556-48.

Silva, W.J. (1992). "Factors controlling strong ground motions and their associated uncertainties." *Seismic and Dynamic Analysis and Design Considerations for High Level Nuclear Waste Repositories, ASCE* 132-161.

Wald, D.J. and T. I. Allen (2007). "Topographic slope as a proxy for seismic site conditions and amplification." *Bull. Seism. Soc. Am.,* 97(5), 1379-1395.

Walling, M., W. Silva and N. Abrahamson (2008). "Nonlinear site amplification factors for constraining the NGA models." *Earthquake Spectra,* 24(1), 243-255.

Wills, C. J. and K. B. Clahan (2006). "Developing a map of geologically defined site-condition categories for California." *Bull. Seism. Soc. Am.*, 96(4A), 1483-1501.

Wills, C.J. and W.J. Silva (1998). "Shear-wave velocity characteristics of geologic units in California." *Earthquake Spectra*, 14(3), 533-556.

Yong, A., S.E. Hough, A. Braverman, and J. Iwahashi (2010). "A terrain-based Vs30 estimation map of the contiguous United States." *Seism. Res. Letters,* 81(2), 294.

Table xx.1a Suite of Hard Rock Peak Accelerations, Source Epicentral Distances, and Depths (**M** 6.5; 1-corner source model)		
Expected Peak Acceleration (%g)	Distance (km)	Depth (km)
1	230.00	8.0
5	74.00	8.0
10	45.00	8.0
20	26.65	8.0
30	18.61	8.0
40	13.83	8.0
50	10.45	8.0
75	4.59	8.0
100	0.0	7.0
125	0.0	5.6
150	0.0	4.7

Additional parameters used in the point-source model are:

$\Delta\sigma$ (1-corner) = 110 bars
ρ = 2.71 cgs
β = 3.52 km/s
R_C = 60 km, crossover hypocentral distance to $R^{-0.5}$ geometrical attenuation
$T = 1/f_c + 0.05\ R$, RVT duration, R = hypocentral distance (km)
Q_o = 670
η = 0.33
kappa(s) = 0.006

Generic Hard Rock Crustal Model		
Thickness (km)	V_S (km/sec)	ρ (cgs)
1	2.83	2.52
11	3.52	2.71
28	3.75	2.78
--	4.62	3.35

Table xx.1b Suite of Hard Rock Peak Accelerations, Source Epicentral Distances, and Depths (**M** 6.5; 2-corner source model)		
Expected Peak Acceleration (%g)	Distance (km)	Depth (km)
1	230.00	8.0
5	81.00	8.0
10	48.00	8.0
20	28.67	8.0
30	20.50	8.0
40	15.60	8.0
50	12.10	8.0
75	6.30	8.0
100	0.0	7.9
125	0.0	6.4
150	0.0	5.4

Table xx.2 Site Independent Relative Weights and Epistemic Uncertainty		
Parameter	Relative Weight	σ_μ
Mean Base-Case Profile	0.40	0.35
Lower-Range	0.30	
Upper-Range	0.30	
Mean Base-Case Kappa	0.40	0.40
Lower-Range	0.30	
Upper-Range	0.30	
G/Gmax and Hysteretic Damping Curves		0.15*, 0.30**
Soil		
EPRI Cohesionless Soil	0.5	
Peninsular Range	0.5	
Firm Rock		
EPRI Rock	0.5	
Linear	0.5	

*Modulus variability at cyclic shear strain 3 x 10^{-2}%
**Shear-wave damping variability at cyclic shear strain 3 x 10^{-2}%

Table xx.3 Maximum Number of Models to Characterize Epistemic Uncertainty				
Parameter	Maximum	Soil	Firm Rock	Soil/Firm Rock
	N	N	N	N
Profile	3	3	3	3
Curves	2	2	2	2
kappa	3	1	3	3
Magnitude	2	1	1	1
1, 2-Corner	2	2	1	2
Total Models	**72**	**12**	**18**	**36**

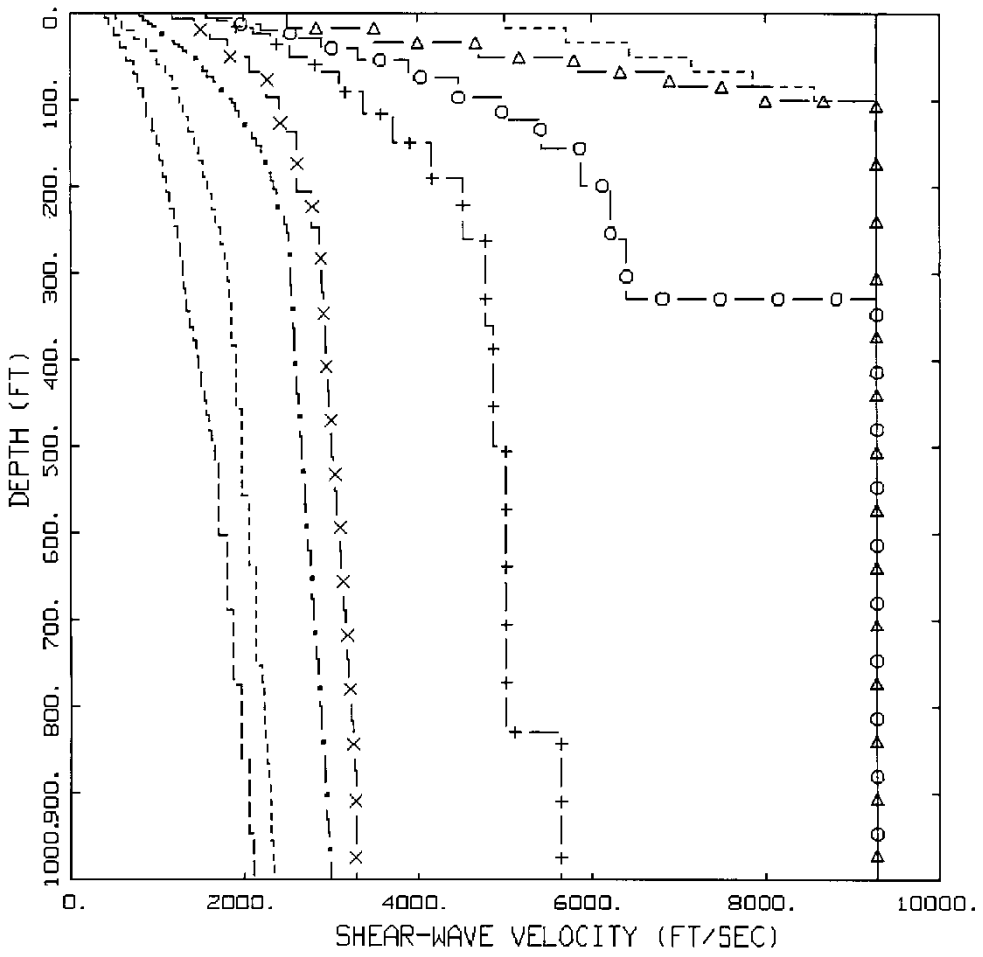

Figure xx.1. Template shear-wave velocity profiles for soils, soft rock, and firm rock. Rock profiles include shallow weathered zone.

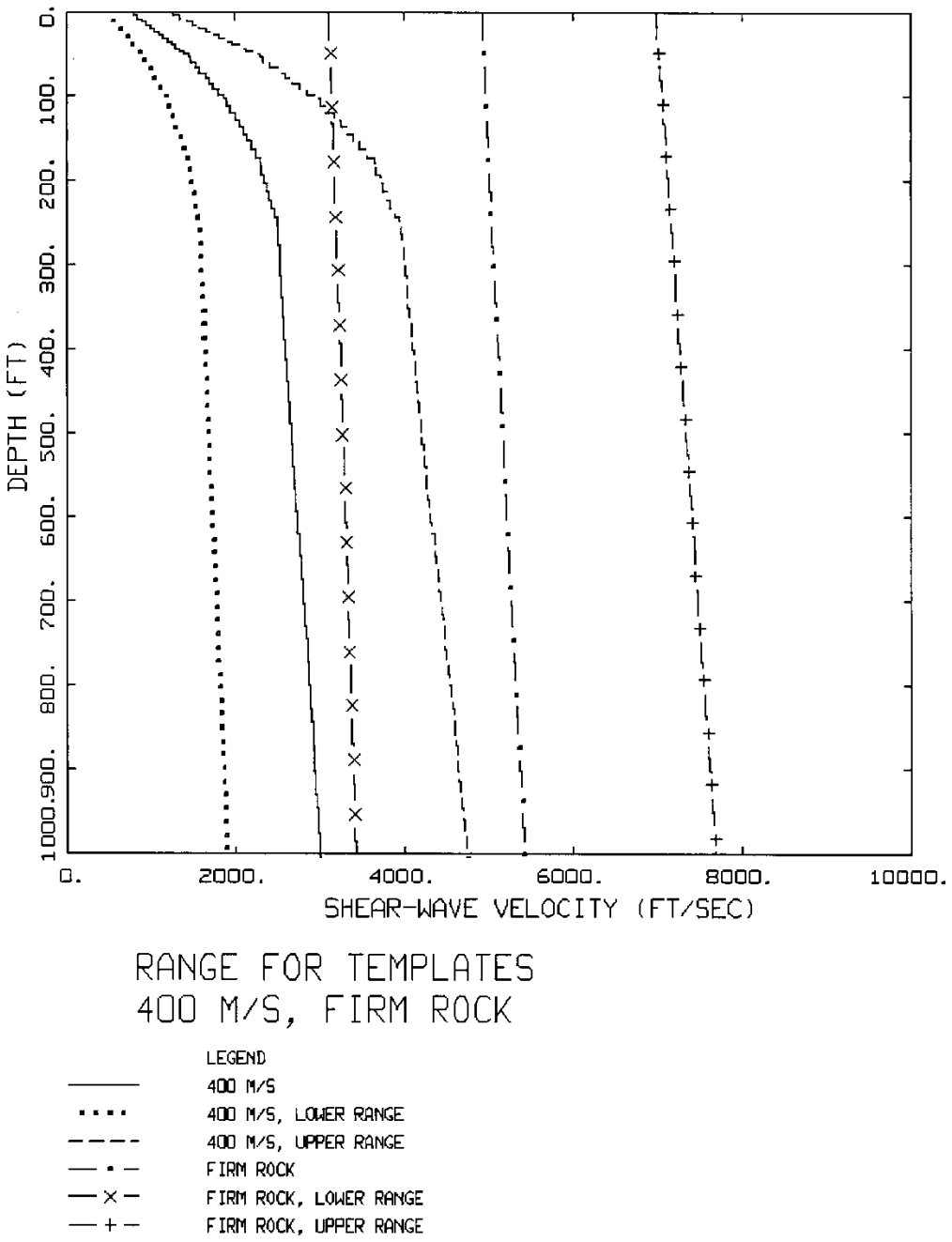

Figure xx.2a. Illustration of the upper range and lower range base-case profiles adopted to accommodate epistemic uncertainty of the mean base-case: 400m/s mean base-case (Figure xx.1) and firm rock (weathered zone removed) taken as 5,000 ft/s at the surface, empirical gradient adopted from Fukushima et al. (1995). Range is a maximum and reflects cases with

few or no measured shear-wave velocities.

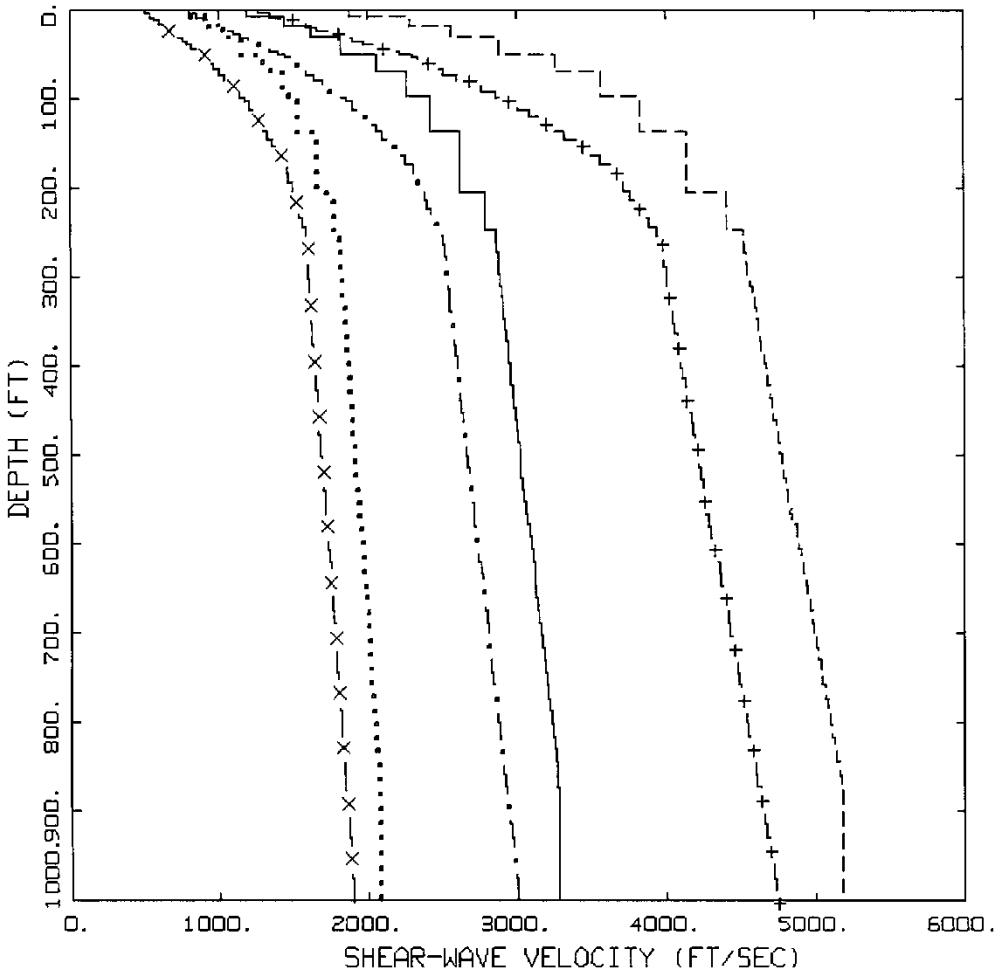

Figure xx.2b. Similar to xx.2a but illustrates maximum ranges for soil templates 400m/s and 560m/s (Figure xx.1).

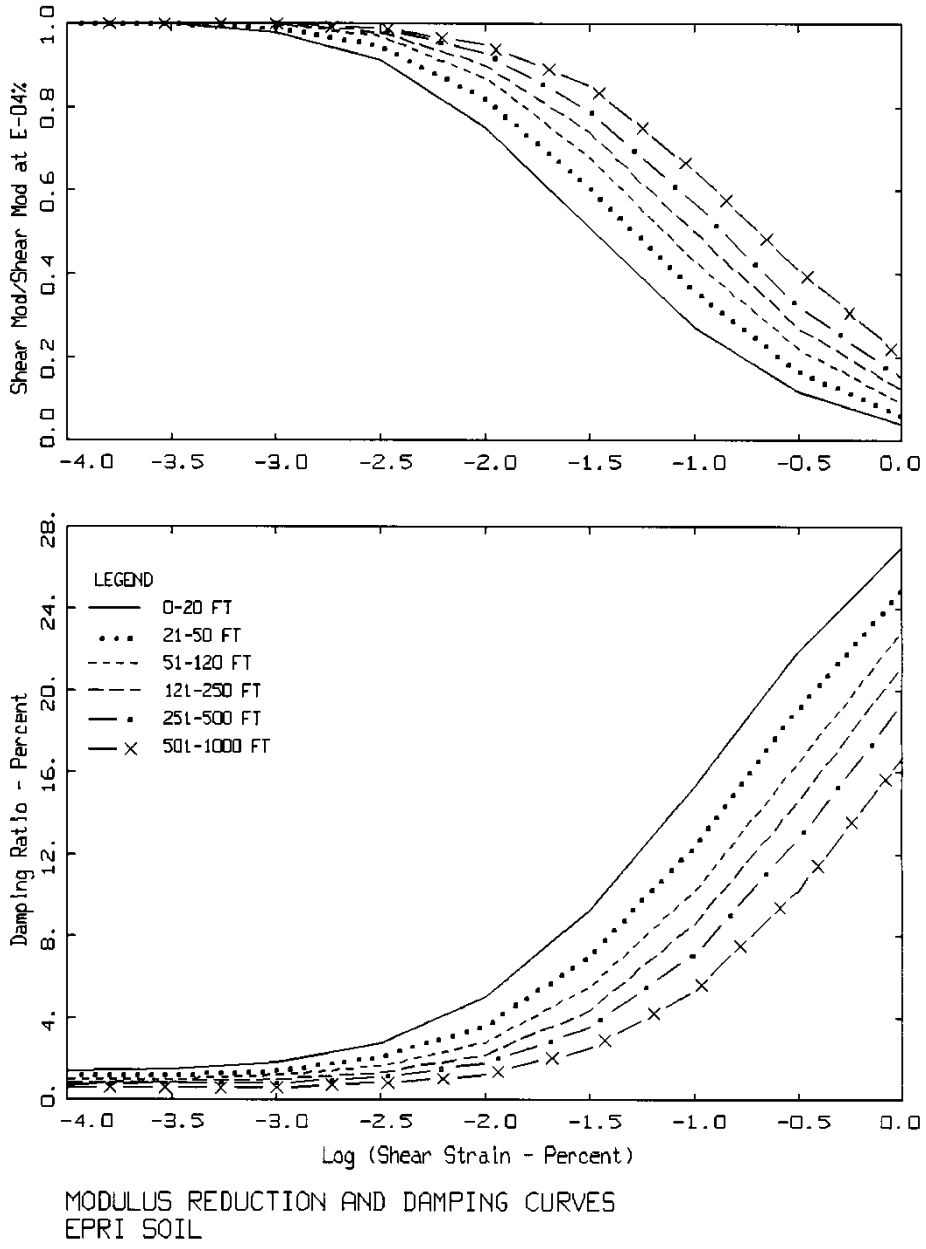

Figure xx.3. Generic G/G_{max} and hysteretic damping curves for cohesionless soil (EPRI, 1993). Damping limited to 15% in application.

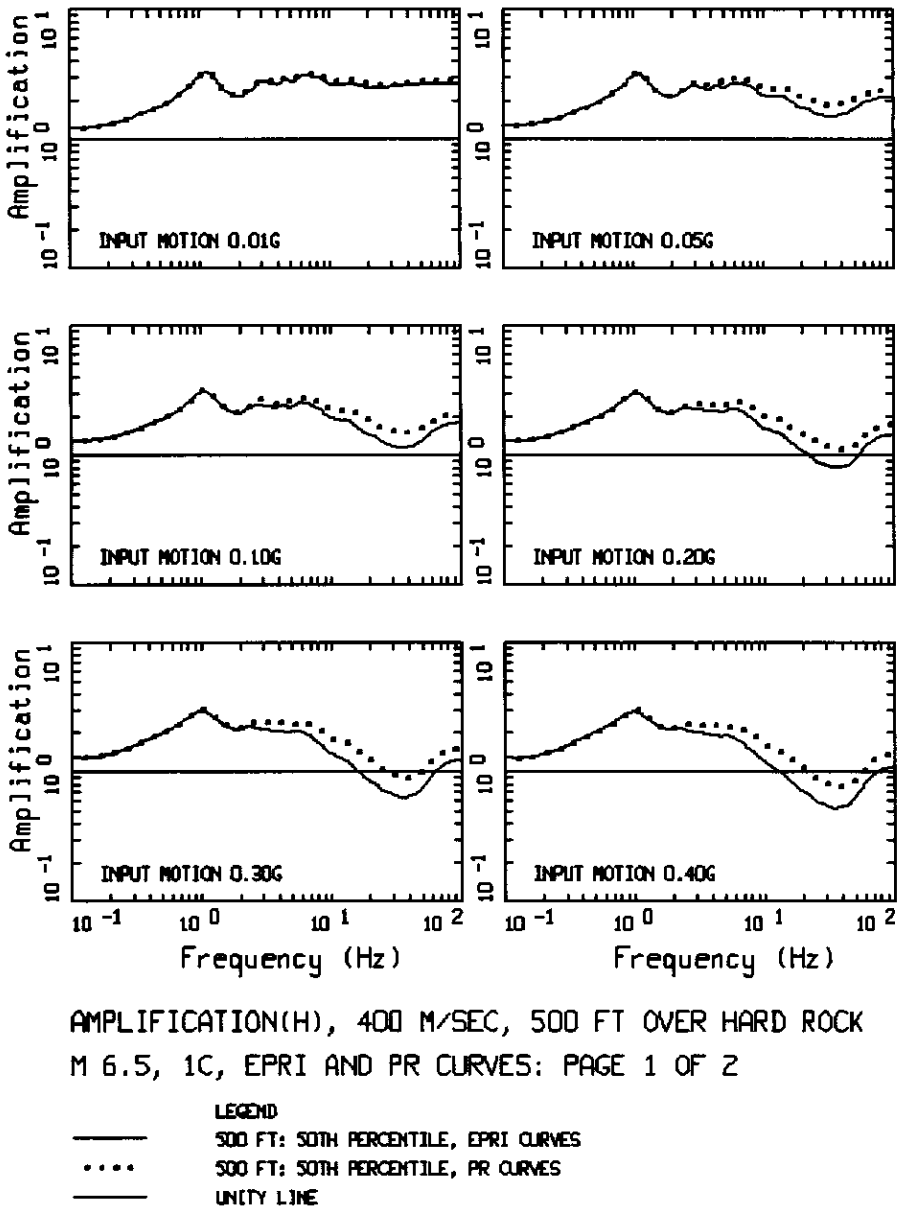

Figure xx.4. Comparison of amplification (5% damped PSa) computed using EPRI (1993) (Figure xx.3) and Peninsular Range (Silva et al., 1996) G/Gmax and hysteretic damping curves, profile 400m/s (Figure xx.2), and the single-corner source model (Table xx.1a). Reference rock loading levels of 0.01g to 1.50g.

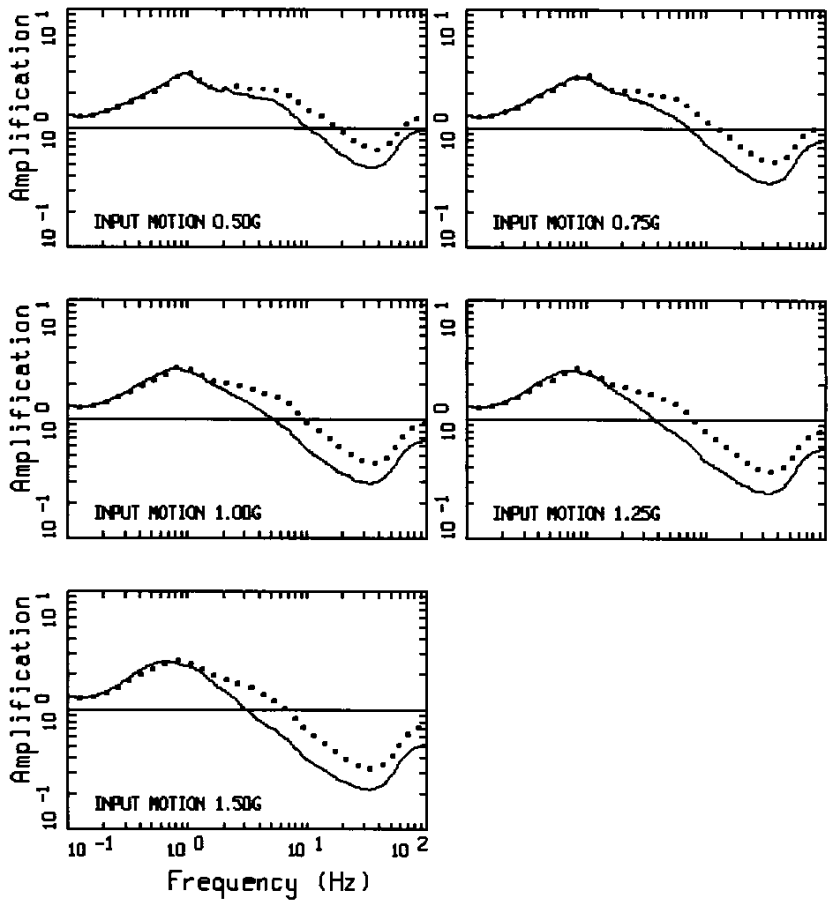

Figure xx.4. (cont.)

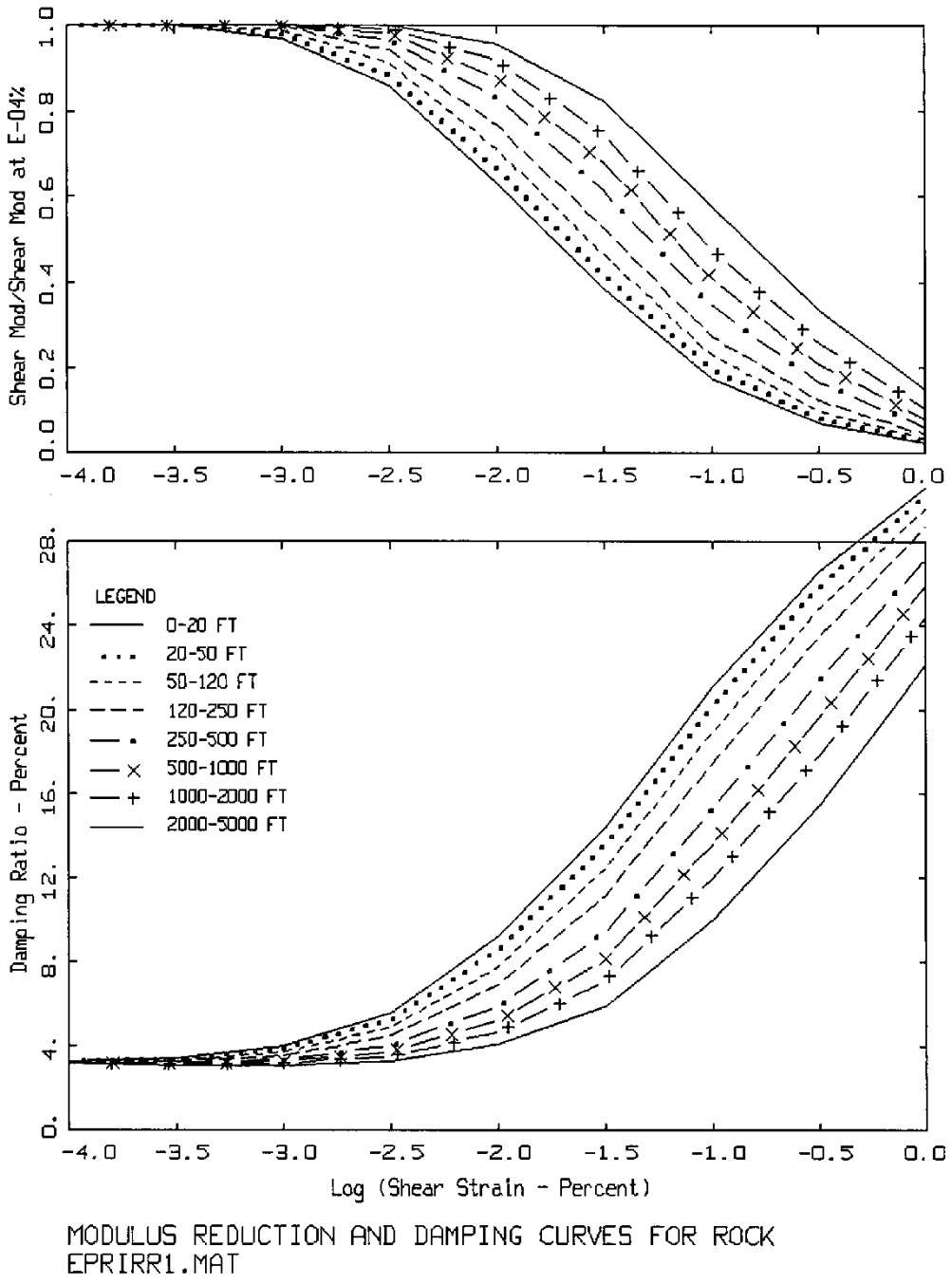

Figure xx.5. Generic G/G_{max} and hysteretic damping curves for firm rock (developed by Dr. Robert Pyke). Damping limited to 15% in application.

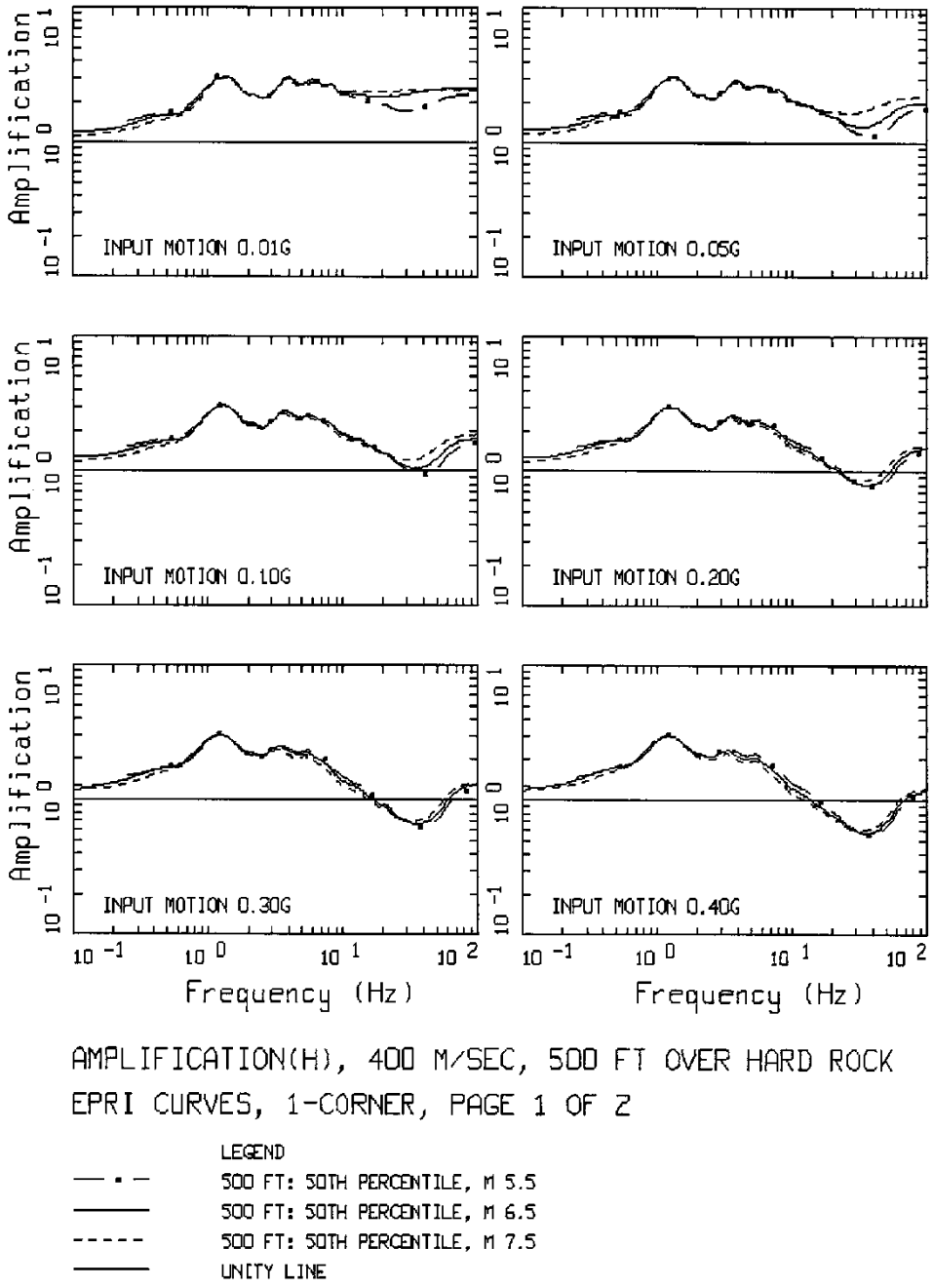

Figure xx.6. Comparison of amplification (5% damped PSa) computed using the single-corner source models (Table x.1a) for stiff soil profile 400m/s (Figure xx.1) and EPRI (1993) G/G_{max} and hysteretic damping curves (Figure xx.4) using **M** 5.5, 6.5, and 7.5. Reference rock loading

levels of 0.01g to 1.50g (Table xx.1).

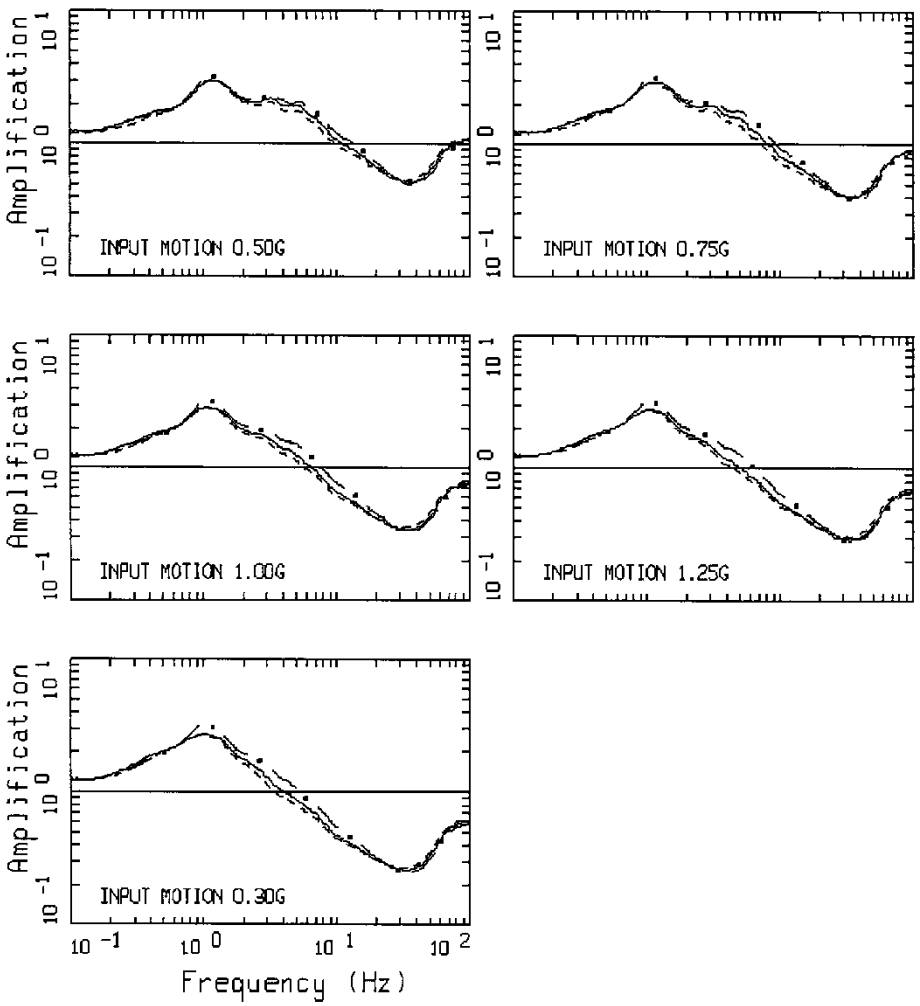

Figure xx.6. (cont.)

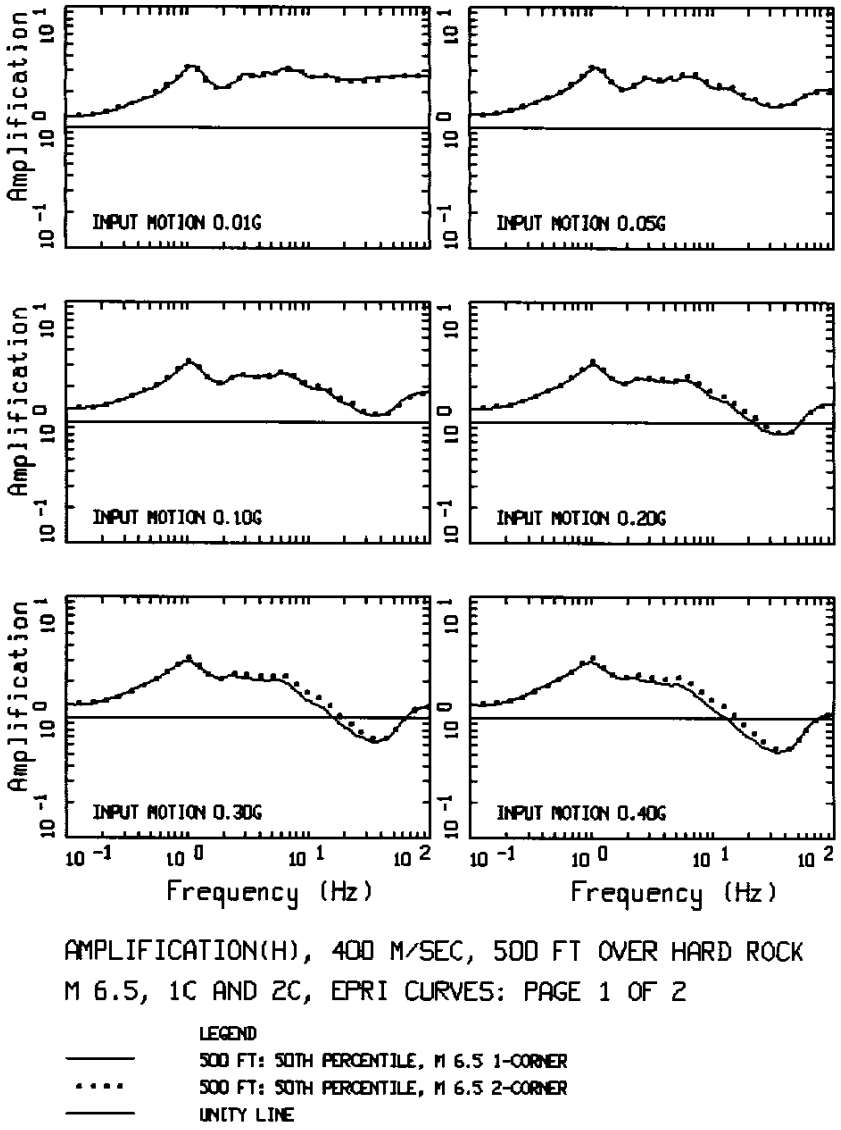

Figure xx.7. Comparison of amplification (5% damped PSa) computed using the single- and double-corner source models (Table x.1a) for stiff soil profile 400m/s (Figure xx.1) and EPRI (1993) G/G_{max} and hysteretic damping curves (Figure xx.4). Reference rock loading levels of

0.01g to 1.50g (Table xx.1).

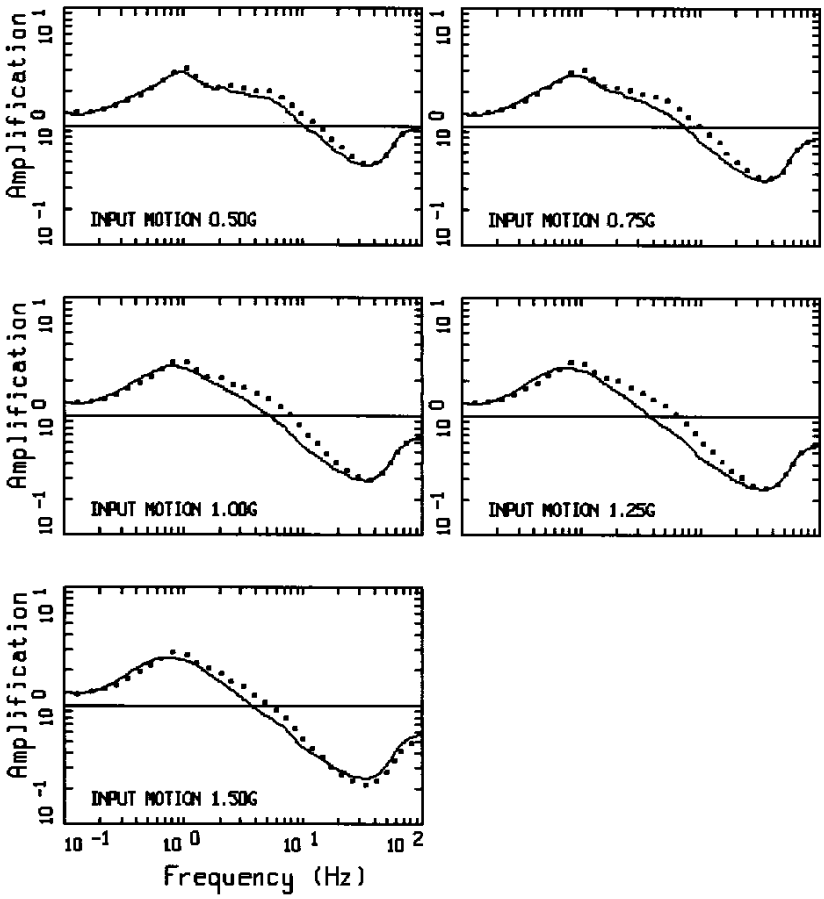

Figure xx.7. (cont.)